Egypt. J. Chem. **Vol. 66**, No. 1 pp. 387 - 398 (2023)

Egyptian Journal of Chemistry

http://ejchem.journals.ekb.eg/

Synthesis and physicochemical characterization of Schiff base complexes and examination of their selectivity index for breast and colon cancer cells.

Rania H. Taha[1,2,*], Esmail M. El-Fakharany[3,*], Zienab A. El-Shafiey[2], Aida A. Salman[2], Mai M. Mansour[2], Mohamed Yahia[4,*].

[1]*Chemistry Department, College of Science, Jouf University, P.O. Box: 2014, Sakaka, Saudi Arabia.*
[2]*Department of Chemistry, Faculty of Science (Girls), Al-Azhar University, P.O. Box: 11754, Yousef Abbas Str., Nasr City, Cairo, Egypt.*
[3]*Protein Research Department, Genetic Engineering and Biotechnology Research Institute (GEBRI), City of Scientific Research & Technological Applications (SRTA-City), New Borg El-Arab City, P.O. Box: 21934, Alexandria, Egypt.*
[4]*Department of Chemistry, Faculty of Science, Helwan University, Ain-Helwan, 11795 Cairo, Egypt.*

Abstract

The present investigation relates to the new method of preparing schiff base of 4-(2-Hydroxy-1,2-diphenyl-ethylideneamino)-1,5-dimethyl-2-phenyl-1,2-dihydropyrazol-3-one as well as the preparation of metallic compounds with certain ions such as (La(III), Gd(III), Co(II), and Cd (II)) in normal and nano-size and their biological applications of their ability to treat colon and breast cancer cells without affecting normal cells. These synthesized compounds have been characterized using different analytical techniques including physicochemical studies such as elemental analysis, electrical conductivity, Uv-visible, IR, nuclear magnetic resonance (NMR), mass spectrometry, magnetic and thermal studies as well as imagining using transmission electron microscopy (TEM). In vitro, the anti-cancer activity of these synthesized compounds was investigated, and their mechanism of action was detected. The results proved that these compounds have the anti-cancer activity against colon cancer (Caco-2) and breast cancer (MCF-7) cell lines at very low concentrations up to 8.27 mg/ml. It was found that the Cd (II) compound showed the highest selectivity against cancer cells without affecting the normal (Vero) cells with selective index (SI) values about 62 times for breast cancer cells and about 51 times for colon cancer cells.

Keywords: Schiff base; 4-aminoantipyrine; metallic compounds; physicochemical studies; anti-cancer activity; apoptosis.

1. Introduction

Due to their important applications in biochemical, biological, catalytically, analytical and industrial field, Schiff base and its metal complexes derived from 4-aminoantipyrine are essential [1]. The presence of N and different donor atoms in the structure makes it biologically active [2]. Recent literature has explained the biological importance of different structural derivatives of heterocyclic compounds. Schiff bases which are the condensed products of aromatic amines and aromatic aldehydes, are notable to possess a large variety of biological applications such as medicine, antifungal, antitumor, analgesic and anti-inflammatory activities [3–5]. Moreover, Schiff bases obtained from varied heterocyclic scaffolds cover a large range of pharmacologic potential like antimicrobial [6], anthelmintic, analgesic [7], anti-inflammatory, allergic inhibitors reducing activity [8], antipyretic [9], diuretic, hypoglycemic [10], antiepileptic drug [11], anti-HIV [12], cytotoxic [13], antitumour [4,14], activities. additionally, determined that radical scavenging [15] anti-oxidative action [16]. Tumor is a multi-step progressive illness, in which some of

*Corresponding author e-mail: mhmd_mosad@yahoo.com ; rhaly@ju.edu.sa; (Rania H. Taha), mohamed.yahia@science.helwan.edu.eg ; Yahia_sci@yahoo.com; (Mohamed Yahia).
Receive Date: 23 January 2022, Revise Date: 13 March 2022, Accept Date: 30 March 2022.
DOI: 10.21608/EJCHEM.2022.117920.5313

cells start proliferating in an abandoned manner as a consequent to a main mutation happens in the cellular genetic. Regulating of cellular genes, cellular proliferation, and cell cycle become mutated and convert the normal cell into tumorous one [17]. These tumor cells evade cell cycle check points, bypass from apoptosis process, progress to form large populations, increase their bulk, and invade nearby tissues [18]. Tumor disease can be detected in persons of all ages and can affect all body cells, tissues, and organs except dead cells such as nails and hair. Tumor disease can be treated and managed efficiently if identified in early stages, however in undiagnosed cases, it could be become fatal and the disease develops to an end stage [19]. There are several types for cancer treatment including chemotherapy, in which tumor cells can resist chemotherapeutics agents, leading to tumor relapsing after an initial treatment. Consequently, the exploring of novel candidates and cure policies to fight this challenge is necessary [20]. Apoptosis is a natural death mechanism for old, injured, or mutated cells that avoids the progressive of tumor, which prevent cancer occurring, and can be enhanced by many types of drugs. Therefore, the stimulation of apoptosis process in tumor cells is a promising objective to achieve a novel agent against numerous types of cancer cells during in vitro and in vivo studies.

Herein, in the present investigation, schiff base of 4-(2-Hydroxy-1,2-diphenyl-ethylideneamino)-1,5-dimethyl-2-phenyl-1,2-dihydropyrazol-3-one and its metal complexes were prepared, characterized and explored for their in vitro anticancer activity on Caco-2 and MCF-7 tumor cells, while cytotoxicity on normal cells was estimated on Vero cells using an MTT method. Capability of these complexes to induce a pro-apoptotic mechanism were detected by using cell cycle analysis and fluorescence microscopy.

2. Experimental and materials.

2.1. Materials and characterizations techniques

Benzoin, 4-amino antipyrine, $CoCl_2$. $6H_2O$, $CdCl_2.H_2O$, $La(NO_3)_3$. $6H_2O$, $Gd(NO_3)_3.6H_2O$, and ethanol, etc. were used with purify (Sigma Aldrich, 98%) and no further purification was required. the elemental analysis (C, H, N, S) were performed using EL-elemental analyzer. The infrared spectra were recorded as pot. bromide discs employing a Perkin-Elmer 437 FTIR spectroscope (400-4000 cm^{-1}). Mass spectra were recorded at seventy heat unit and three hundred 0C on a Hewlett-Packard spectroscope model MS 5988. The proton-HNMR spectra (DMSO – d6) were recorded on a Pruker FT-400MHZ spectrometer. Electronic (UV-visible) spectra were recorded on a Schimadzu UV-spectrophotometer within the vary (200-800 nm). Thermal analyses were administrated using thermal gravimetric analysis analyzer TGA-50 SHIMA VZU and DTA, TA50 Shimadzu in dynamic N atmosphere with a heating rate 10^oC/ min. The magnetic susceptibility measurements of the complexes were administrated using Gouy balance. The conductivity was measured on JEN method 4510 conductivity meter at room temperature. Electron microscopes (SEM) and (TEM) techniques were used to determine the particle nanosize and % in complexes, the sample was coated with gold and the patterns were performed with (CuKα radiation).

2.2. Synthesis of Schiff base ligand

The ligand in **Fig .1** was prepared by the ordinary ways [21]. To the ethanolic solution of benzoin (5.30 g, 0.025 mol) an ethanolic solution of 4-amino anti pyrine (5.08 g, 0.025 mol) was added (with an equi molar ratio), the reaction mixture was heated under fluxed for 4hs in a water bath. The product was cooling and collected by filtration, washed many times with alcohol and ether then dried in a desiccator over anhydrous salt to provide 61.62% of an orange powder the ligand.

2.3 Synthesis of metal complexes in bulk size

The metal complexes were synthesized by the addition of (0.0025 mol) of the ethanolic solution of La $(NO_3)_3.6H_2O$, or $Gd(NO_3)_3.6H_2O$, $CoCl_2.6H_2O$, $CdCl_2.H_2O$ to a hot ethanolic solution of the ligand (0.0025 mol). Then the mixture was stirred and refluxed for two hr. the product was filtered, washed with alcohol and ether then dried in a desiccator over anhydrous salt [22]. The isolated complexes (1-5) are powder, stable in air, soluble in DMSO and DMF, and their elemental analyses are in good agreement with the proposed structure and the suggested molecular formulae. The analytical data of the complexes and their physical properties are summarized in **table S1** (supporting information (SI)).

2.4. Green chemistry method for synthesis of Gd complex in Nano size

10 cc of a 0.1 M solution of $Gd(NO_3)_3.6H_2O$ in ethanol were positioned in a high-density inaudible probe, in operation at twenty four kilohertz with a most power output of four hundred watt (400 W). Into this solution ten cc of a 0.1 M solution of the ligand was added drop wise. The obtained precipitate was evaporated at room temperature to get Gd complex nano particle in dark Yellow powder [23].

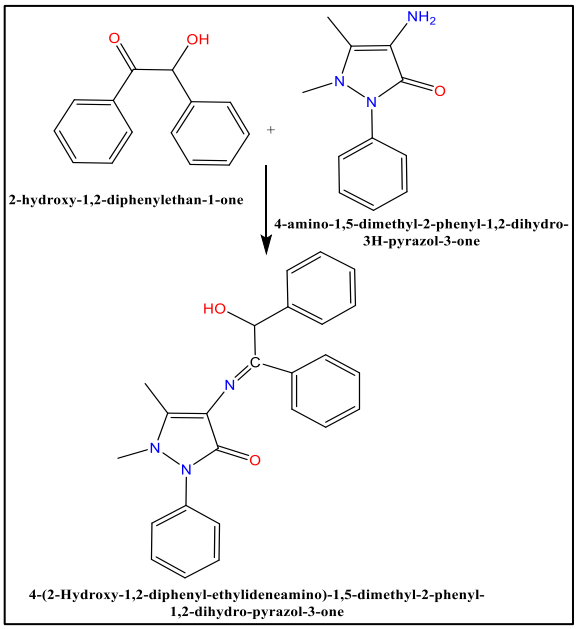

Fig.1. Schematic representation of the bidentate ligand.

2.5. Cytotoxicity of synthesized complexes against normal and cancer cell lines.

The cell viability and cytotoxicity of the synthetic complexes both in bulk and nano size were assessed at different concentrations using normal (Vero) cells, colon carcinoma (Caco-2) cells and breast carcinoma (MCF-7) cells according to El-Fakharany et al. [24] and Mosmann [25]. In brief, both Vero and Caco-2 cell lines at concentration (5×10^3) cells per well in 96 well plate were cultured in DMEM medium supplemented with 10% of fetal bovine serum (FBS) and 100 units/ml penicillin/streptomycin, while MCF-7 cells were cultured in RPMI-1640 medium supplemented with 10% of FBS and 100 units/ml penicillin/streptomycin. After incubation for 24 h at 5% of CO_2 at 37°C and 88% humidity, the synthesized compounds at final concentrations of 10-1000 µg/ml in 200 µl total volume of used supplemented medium per well.. After incubation the cells for 24 h in 5% CO_2 incubator, dead cells and debris were removed by washing three times with PBS, pH 7.2. Aliquots of 200 µL of MTT solution (0.5 mg/ml) was added to each well and incubated at 37ºC and 5% CO_2 for 3-5 h. Formed formazan crystals were dissolved in 200 µl DMSO and shook for 5 min at 150 rpm, and then OD was measured at 570 nm. The relative of viability cells was determined by comparison with untreated cells as control (100%) using the following equation: (X) test/ (Y) control × 100 [26]. The safe dose (EC100) and half maximal inhibitory concentration (IC50) values of all synthesized complexes that cause 100% and five hundredth cell viability, respectively, were calculated by the Graph-pad prism 6.0 software. The selectivity index (SI) values that outlined because the magnitude relation of the IC50 on normal cells versus tumor cells were also calculated for all synthesized complexes [27].

2.6. Investigation of cell apoptotic effect using phase contrast microscope.

Human colon carcinoma (Caco-2) cells were treated with the synthetic complexes at IC50 concentrations. After incubation for 24 h, Caco-2 and MCF-7 cells were washed 3 times with PBS, fixed with 4% paraformaldehyde for 10 min and permeabilized with 3% paraformaldehyde and 0.5% Triton X-100 for 1 min. After washing with PBS, the cells were stained with propidium iodide (PI; Sigma, USA). Apoptotic effect of the synthetic complexes was visualized under fluorescence phase contrast microscope. The cells with condensed and fragmented nuclei were assessed as apoptotic cells [28,29].

2.7. Flow cytometric analysis.

To determine cell cycle arrest, alteration in cell cycle populations after treatment with the synthetic complexes at different concentrations was investigated by flow cytometry as described by previously with Abu-Serie and El-Fakharany (2017) and El-Fakharany et al. (2020) in comparison with untreated cancer cells. MCF-7 cells were seeded into 12-well plate at density 1.0×105 cells/ml and incubated in 5% CO_2 incubator at 37 °C for 24 h. After that, the cells were treated with the synthetic complexes at IC50 concentrations. After incubation for 24 h, the untreated and treated cells were washed, trypsinized, fixed in 80% cold ethanol and treated with 5 µg/ml RNase A (Sigma, USA). After incubation for 2h, the cells were stained with 10 µg/ml PI for 20 min in dark condition. Cell cycle distribution was measured by flow cytometry (Partec,

Germany) using Mod Fit and Cell Quist softwares at 488 nm within 3 h.

3. Results and discussion

The elemental analysis data and the physical properties of the prepared schiff base ligand and its metal complexes are listed **in table S1** (SI). The elemental analysis data shows that the synthesized compounds have (metal: ligand) stoichiometry with molecular formula $[Co(HL).Cl.3H_2O]$, $[Cd(HL).Cl.3H_2O]$, $[La(HL).(NO_3)_3.H_2O]$, $[Gd(HL).(NO_3)_3.H_2O]$, and $[Gd(HL).(NO_3)_3.H_2O]$ nano. The complexes (1-5) have molar conductance 7.42,1.78,7.17, 1.58 and 7.12 $S.cm^2.\ mol^{-1}$ representing their non-electrolytic nature [23].

3.1. ^{1}H NMR analysis

^{1}H-NMR (**Fig.2**) analysis shows that the ligand provides a singlet peak at 9.42 ppm that attributed to the O-H proton and additionally provides a singlet peak at 3.13 ppm due to CH_3 group. in addition to a multiplet peaks at 7.15-7.72 ppm due to phenyl protons. Upon complexation it had been found that the disappearance of the hydroxyl group proton peak and additionally the CH_3 proton peak shifted to 3.14 ppm and additionally the phenyl protons provide a multiplet peak at 7.15– 7.94 ppm. Indicating the participation of the hydroxyl group in complexation with its deprotonation.

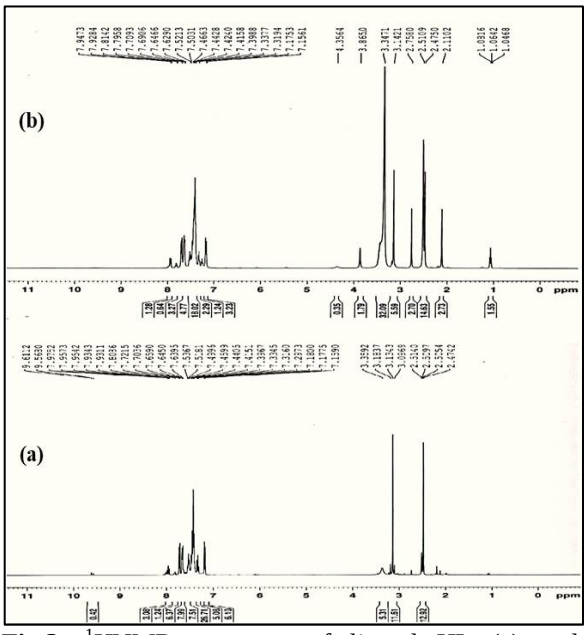

Fig.2. ^{1}HNMR spectrum of ligand HL (a) and cadmium complex $[Cd(HL)Cl.3H_2O]$ (b).

3.2. Infrared spectra

The Infrared interpretation data listed in **table 1** and **Fig.S1** (SI). The peaks at 1590, 1172, and 1662 cm^{-1} in the spectrum of the free ligand are due to azomethine group, C-O, and C=O groups, respectively [31]. The IR spectra of the metal complexes showed that shift within the peaks of C-O, C=N groups because of their participation in complexation and confirmed also by the appearance of new peaks due to M-O, and M-N. The peak due to C=O group does not show any shift indicating that this group does not participate in complexation.

Table 1: Infrared -spectral bands (cm^{-1}) of the Schiff base ligand, (HL) and its meta complexes.

Compd. No.	υC=N	υC=O	υC-O	υM-O	υM-N	υNO_3		
						$\upsilon 1$	$\upsilon 2$	$\upsilon 3$
HL	1590	1662	1172	---	-----	---	---	---
1	1593	1662	1170	692	552	---	---	---
2	1601	1663	1067	698	555	---	---	---
3	1588	1664	1027	697	549	1063	1313	1447
4	1588	1663	1143	698	551	1063	1313	1446
5	1588	1664	1027	697	549	1063	1313	1447

3.3. Mass spectrum

The spectrum of the free ligand, HL (**Fig.3**) shows that the peak at m/z 397.22 (14.68%) that agree with the formula $C_{25}H_{23}N_3O_2$; 397.51. Also, the spectrum shows many different peaks according to other fragments, their intensity provides the stability of the fragments. Furthermore, **Fig.S2** (SI) shows the proposed pathway of the decomposition steps for the ligand.

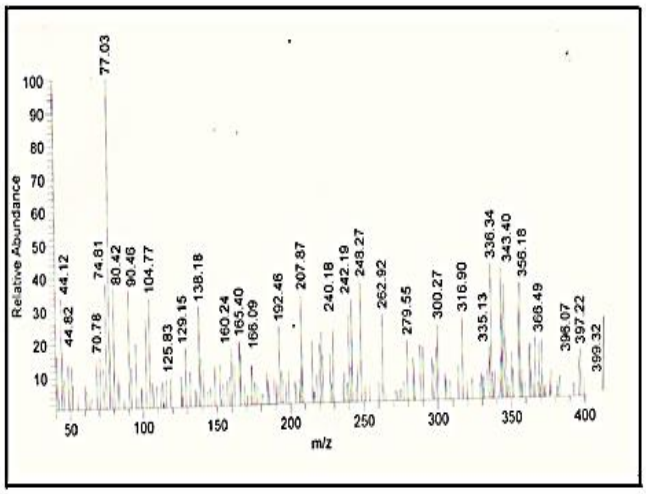

Fig. 3. Mass spectrum for the ligand HL

3.4. Ultraviolet-visible electronic spectra and magnetic susceptibility measurement

Table 2 indicates the transition bands and the magnetic moment values. **Fig.S3 (SI)** shows the electronic spectra of the ligand and its complexes. The ligand shows an absorption bands at 219 and 250 nm due to π→π* and n→π* respectively. Up on complexation, these bands were shifted. Both Cd (II) and La (III) complexes are diamagnetic in nature with no *d-d* transition. In keeping with all previous information and analysis the octahedral structure is also suggested. The electronic spectra of Co (II) complex showed 3 absorption bands at 520, 578, and 642 nm assigned to the transition $4T_{1g}$ (F) $\rightarrow {}^4T_{1g}$(P) and ${}^4T_{1g}(F) \rightarrow {}^4A_{2g}(F)$, and therefore the magnetic moment value is 3.15B.M that confirmed the octahedral structure. The electronic spectrum of Gd complex don't has any transition bands over four hundred nm as a result of forbidden *f-f* transition. The magnetic moment value is 2.66 B.M. confirmed the octahedral structure [23,31].

Table 2: UV spectra for the ligand, HL and its metal complexes.

Compd. No.	μ_{eff} (B.M.)	Absorption bands (nm)		
		π-π*	n-π*	*d-d* transition
HL	-	219	250	---
1	3.15	209	280	520,578,642
2	Diamagnetic		337	---
3	Diamagnetic	290	338	---
4	2.63	298	339	---
5	2.66	296	338	---

3.5. Thermal studies

All data for thermal analysis are listed in **table S2 (SI).** The thermos-gram of the complex [Co(HL).Cl.3H_2O] as **Fig.S4 (SI)** shows that there's a 3 coordinated water molecules. The first stage of decomposition is beginning at 46-211^oC the observed mass loss is 4.63 % because of the loss of 1.5 water molecule. The second stage of decomposition is from 213 ^oC to 440 ^oC the observed mass loss is 25.96% this is because of the loss of 1.5 H_2O, 2HCN, HCl, and CO. the third stage of decomposition is from 441^oC to 693 ^oC. The observed mass loss is 13.60% this is because of the loss of C6H5. The fourth stage is from 694 ^oC to 999 ^oC the observed mass loss is 40.36% is because of the loss of $C_{10}H_7$ and C_6H_7N leaving residue as CoO. The overall mass loss is observed to be 84.55% that is in well agreement with the calculated value 86.22%.

3.6. EDX spectra and TEM analysis

EDX data was used for identifying the amount of elements present in percentage level of the metal complexes. EDX spectra is employed to calculate the % of the elements present within the metal complexes like C, O, N, and Gd that present within the Gd(III) complex (in bulk and nano size) shown within **Fig .4**.

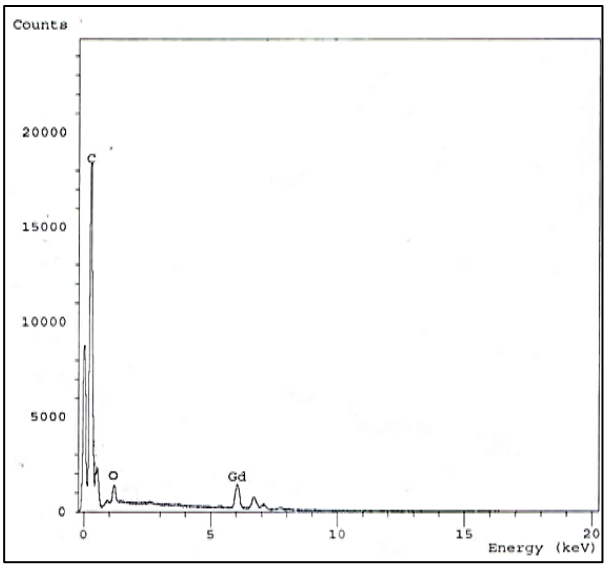

Fig.4. EDX analysis for Gd(III) nano complex.

TEM analysis is performed to examine the size and shape of the nanoparticles. The Gd(III) complex nanoparticle was fairly uniform in size, spherical in shape, and with average diameter starting from 42.91 to 47.32 nm (**Fig.5**), the microscopy analysis allowed to confirm visually the observed stability of the obtained nano complex. The revealed data are in good agreement with that of the elemental analysis [31].

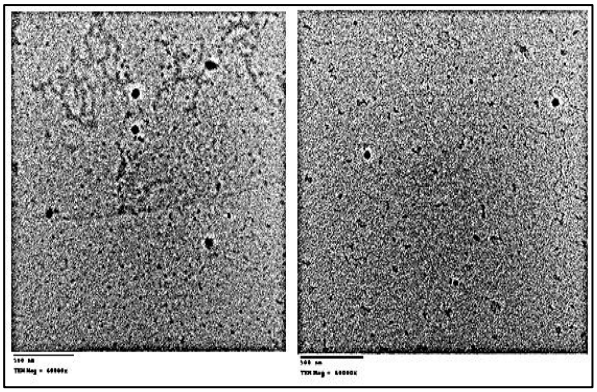

Fig .5. TEM images for Gd(III) nano complex.

Finally, correlation of all techniques employed in characterization of the synthesized complexes provides the proposed structure of the metal complexes as represented in **Fig.S5 (SI).**

3.7. Cytotoxic effect of the synthetic complexes on the normal cells.

The cell viability (%) of the synthetic complexes was investigated in vitro on Vero cells using MTT method. The results are given in **table 3**, which clearly indicates that safe dose (EC100) for complexes HL, 4 and 5 were significantly ($p < 0.001$) higher than the EC100 values determined for complexes 1, 2 and 3. Furthermore, the cell viability was decreased to 50 percent (IC50) at concentrations of 274.71±4.52, 993.73±8.38, 422.12±5.09, 1273±11.24, 521.35±6.23 and 563.56±5.98 µg/ml for complexes HL, 1, 2, 3, 4 and 5, respectively (**table 3**).

Table 3: EC100 (µg/ml) and IC50 (µm/ml) values for effect of the synthetic complexes on normal epithelial (Vero) cells.

compound number	EC_{100}	IC_{50}
HL	4.44±0.56	274.71±4.52
1	0.04±0.01	993.73±8.38
2	0.33±0.04	422.12±5.09
3	0.06±0.01	1273.00±11.24
4	17.07±0.71	521.35±6.23
5	35.38±0.37	563.56±5.98

3.8. Cytotoxic effect of the synthetic complexes on cancer cell lines.

In vitro cytotoxicity of the synthetic complexes was estimated by MTT method using colon and breast cancer cell lines after treatment for 24 h. Both Caco-2 and MCF-7 cells were exhibited a strong sensitivity toward the synthetic complexes at low concentrations. Based on IC50 and SI results (shown in **table 3**), complex 2 showed the highest anticancer effect against Caco-2 and MCF-7 cells with IC50 values of 8.27±0.69 and 6.79±0.54 µg/ml and SI values of 51.04 and 62.17, respectively. In general, MCF-7 cell line was more sensitive to the treatment with complexes 1, 2 and 4 than Caco-2 cell line, whereas Caco-2 cells were more sensitive to the treatment with complexes HL, 3 and 5 than MCF-7 cells.

3.8. Analysis of anticancer activity

Investigation of cell cycle phases of Caco-2 cells was analysed to detect the apoptotic effect and anti-tumor mechanisms of the synthetic complexes in vitro using flow cytometry. **Fig.6** shows the results of the cell cycle population's analysis for Caco-2 cells before and after treatment with the synthetic complexes at their IC50 concentrations. **Fig.6** demonstrates that the percentage of both resting state/first growth synthesis (G0/G1) and second growth synthesis/mitosis (G2/M) phases was around 89% in untreated (control) Caco-2 cells, while these phases were reduced significantly after treatment with all complexes at their IC50 doses for 24 h. The sub-G1 populations were observed and became dramatically detected, demonstrating the synthetic complexes were capable to induce apoptosis mechanism. Furthermore, all tested complexes have the ability to suppress the populations of both G2/M and S phases (Fig. 6a and 6b).These findings indicated that all tested complexes induced to arrest Caco-2 cells in both G2/M and S phases of cell cycle distribution causing apoptosis in tumor cells. In addition, anti-tumor mechanism of these complexes was also determined by nuclear staining method using Propidium iodide (PI) dye as fluorescent intercalating agent. PI bind to DNA fragments forming DNA-PI complexes which make the nucleus of the treated cells appears with highly fluorescent under fluorescence microscopy and become easily detectable. **Fig.6c** shows that all tested complexes were able to induce apoptosis to the treated Caco-2 cells. It is detected from the photomicrograph that the Caco-2 cells became more round and lose their normal spindle shape after treatment with the synthetic complexes for 24 h at IC50 doses, as compared to untreated cells. Furthermore, **Fig.6c** shows that the chromatin became fragmented and the nuclei was more condensed, however the untreated cells were characterized by a normal cell shape and intact nuclei, and that these effects more detectable in case of treatment with complexes 2 and 3 than those caused by the treatment with complexes. From the present study, it can be inferred that Cd(II) complex $[Cd(HL)Cl.3H_2O]$, is a potent anticancer candidate which is pretty in agreement with our previous study [13,31].

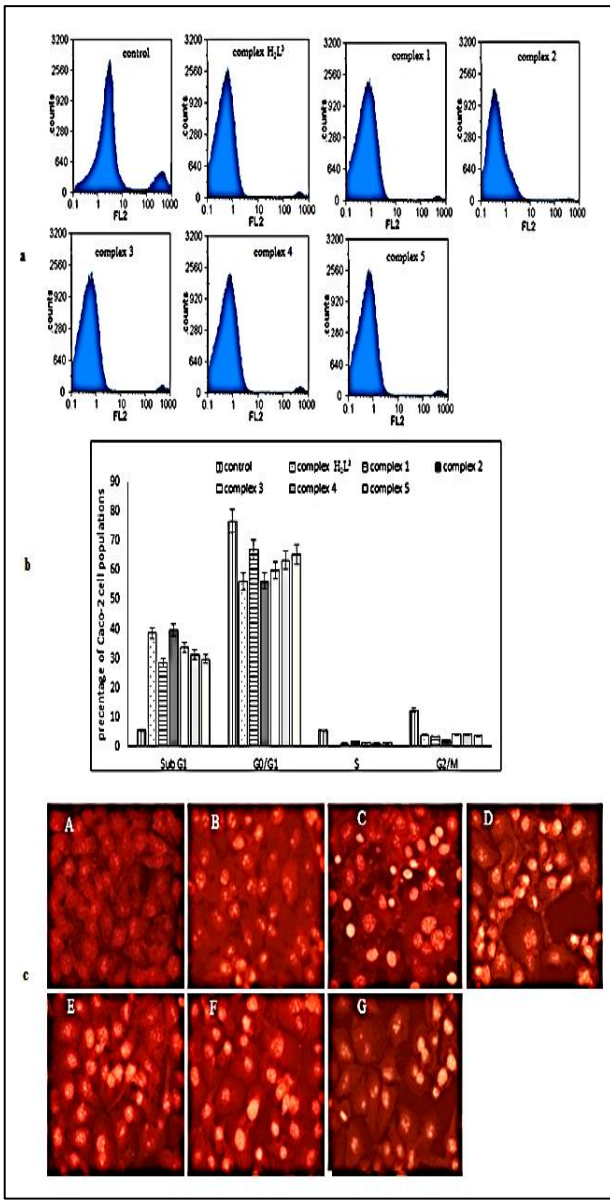

Fig. 6. Analysis of cell cycle distribution and apoptotic effect of the synthetic complexes on Caco-2 cancer cell line. Flow charts of cell cycle analysis before and after treatment with the synthetic complexes for 24 h (a), quantitative distribution of Caco-2 cell cycle populations in different phases after treatment in comparison with untreated cells as control cells (b) and fluorescence photographs of Caco-2 cells stained with PI dye under a phase contrast microscope after treatment with the synthetic complexes for 24 h (c). (A) Untreated "control" cells and (B-G) cells exposed to IC50 (µg/ml) of complexes HL, 1, 2, 3, 4 and 5, respectively.

4. Conclusion

The prepared Schiff base ligand from 4-aminoantipyrine and its prepared metal analogues both in bulk and nano size were synthesized and characterised using various techniques. The findings of the antitumor activity revealed that the complex of Cd(II) exhibited a significant nontoxic behaviour and higher selectivity against both colon and breast tumour cells, sparing normal cells. It is essential that the anti-tumor activity of this Schiff base should be concluded for further in vivo investigations using animal models for use these prepared bulk and nano compounds as promising candidates in medicine for fighting different types of cancers.

Conflicts of interest

The authors declare that there is no conflict of interest regarding the publication of this paper.

Data availability statement

Data sharing not applicable to this article as no datasets were generated or analysed during the current study.

Acknowledgment

The author gratefully acknowledges the financial support from Jouf University (Saudi Arabia), Al-Azhar University (Egypt), and SRTA-City (Egypt).

5. References

[1] Palanimurugan A, Dhanalakshmi A, Selvapandian P, Kulandaisamy A, Electrochemical behavior, structural, morphological, Calf Thymus-DNA interaction and in-vitro antimicrobial studies of synthesized Schiff base transition metal complexes, Heliyon. (2019). doi:10.1016/j.heliyon.2019.e02039.

[2] Liu C.M , Xiong R.G, You X.Z., Liu Y.J, Cheung K.K, Crystal structure and some properties of a novel potent Cu_2Zn_2SOD model Schiff base copper(II) complex $\{[Cu(bppn)](ClO_4)_2\}_2 \cdot H_2O$, Polyhedron. (1996). doi:10.1016/0277-5387(96)00163-5.

[3] Kumar S., Kadadevar D., Synthesis and Antimicrobial Study of Some Schiff Bases of Sulfonamides, J Current Pharma Res. (JCPR) (2010).

[4] Kumar S., Priya Matharasi D., Gopi S., S. Sivakumar, Narasimhan S., Synthesis of cytotoxic and antioxidant Schiff's base analogs of aloin, J Asian Nat Prod Res. (2010). doi:10.1080/10286021003775327.

[5] El-Shafiey Z.A., El-Wahab Z.H., A.A. Salman, Taha R.H., Study of binary and ternary complexes of Co(ii), Ni(ii), Cd(ii), Fe(iii), and UO_2(II) complexes of amino carboxylic acid derivatives and pyridine, synthesis, spectroscopic characterization, thermal investigation and biological activity, Egypt J Chem. (2010). doi:10.21608/ejchem.2010.1211.

[6] Gupta V., Sanchita S., Gupta K.Y., Synthesis and Antimicrobial Activity of some Salicylaldehyde Schiff bases of 2-aminopyridine, J.Chem.Res. 3, 26-29, (2013).

[7] Latha K., Vaidya V., Keshavayya J., Synthesis, characterization and biologicalinvestigations on metal complexes of 2-acetyl naptha (2,1-b) furan semicarbazone, J Teach Res Chem. 11, 39-48, (2004).
[8] Hadjipavlou-Litina D.J., Geronikaki A.A., Thiazolyl and benzothiazolyl Schiff bases as novel possible lipoxygenase inhibitors and anti inflammatory agents. Synthesis and biological evaluation, Drug Des Discov. (1998).
[9] Valli G., Ramu K., Mareeswari P., Thanga Thirupathi A., Anti-inflammatory, CNS and Insilico drug activities of 2-((4-Hydroxyphenylimino) methyl) phenol schiff base, Res J Pharm Technol. (2012).
[10] Lautre H.K., Das S., Patil K., Youssouffi H., T. Ben Hadda, A.K. Pillai, Evaluation of Antimicrobial and Diuretic Activity of Schiff Base Metal Complexes, Part-I, Lautre et Al. World J Pharm Pharm Sci. (2014).
[11] Mohammed Khan K., Rahim F., Ambreen N., Taha M., Khan M., Jahan H., Najeebullah H., Shaikh A., Iqbal S., Perveen S., Iqbal Choudhary M., Synthesis of Benzophenonehydrazone Schiff Bases and their In Vitro Antiglycating Activities, J. Med. Chem. (2013). doi:10.2174/1573406411309040013.
[12] Pandeya S.N., Rajput N., Synthesis and anticonvulsant activity of various Mannich and schiff bases of 1,5-benzodiazepines, Der Pharmacia Lettre. (2012). doi:10.1155/2012/237965.
[13] Taha R.H., Saleh N.M., Elhady H.A., Khodairy M.M., Evaluation of newly synthesized derivatives of bis(hydrazine-1-carbothioamide) and their metal complexes synthesized in bulk and nano size as potent anticancer agents, Appl Organomet Chem. (2019). doi:10.1002/aoc.5207.
[14] Sunil D., Isloor A.M., Shetty P., Nayak P.G., Pai K.S.R, Fun H.K., Corrigendum to In vivo anticancer and histopathology studies of Schiff bases on Ehrlich ascitic carcinoma cells, Arab. J. Chem. 6(1) 25-33, (2013). doi:10.1016/j.arabjc.2013.01.007.
[15] Qiao X., Ma Z.Y., Xie C.Z., Xue F., Zhang Y.W., Xu J.Y., Qiang Z.Y., Lou J.S., Chen G.J., Yan S.P., Study on potential antitumor mechanism of a novel Schiff Base copper(II) complex: Synthesis, crystal structure, DNA binding, cytotoxicity and apoptosis induction activity, J. Inorg. Biochem. (2011), doi:10.1016/j.jinorgbio.2011.01.004.
[16] Mohammed Khan K., Taha M., Naz F., Siddiqui S., Ali S., Rahim F., Perveen S., Iqbal Choudhary M., Acylhydrazide Schiff Bases: DPPH Radical and Superoxide Anion Scavengers, J. Med. Chem. (2012). doi:10.2174/157340612801216111.
[17] I.J. Hyndman, Review: the Contribution of both Nature and Nurture to Carcinogenesis and Progression in Solid Tumours, Cancer Microenviron. (2016). doi:10.1007/s12307-016-0183-4.
[18] Kim S., New and emerging factors in tumorigenesis: An overview, Cancer Manag. Res. (2015). doi:10.2147/CMAR.S47797.
[19] Virnig B.A., Baxter N.N., E.B. Habermann E.B., Feldman R.D., Bradley C.J., A matter of race: Early-versus late-stage cancer diagnosis, Health Aff. (2009). doi:10.1377/hlthaff.28.1.160.
[20] Cree I.A., Charlton P., Molecular chess? Hallmarks of anti-cancer drug resistance, BMC Cancer. (2017). doi:10.1186/s12885-016-2999-1.
[21] Kumar K.V., Sunand K., Ashwini K., Kumar P.S., Vishnu S., Samala A., Synthesis characterization and antibacterial studies of 4-aminoantipyrine schiff's bases, International J. Appl. Pharm. Sci. Res. 2, 8–14. (2017), http://dx.doi.org/10.21477/ ijapsr.v2i1.6908.
[22] Jansi R, SYNTHESIS AND CHARACTERIZATION OF SCHIFF BASE METAL COMPLEXES DERIVED FROM 3-ETHOXYSALICYLALDEHYDE AND 2-AMINO-4-METHYL PHENOL, World J Pharm Pharm Sci. 5, 895–904 (2016).
[23] Aly H.M., Taha R.H., El-Deeb N.M., Alshehri A, Efficient procedure with new fused pyrimidinone derivatives, Schiff base ligand and its la and Gd complexes by green chemistry, Inorg. Chem. Front. (2018). doi:10.1039/c7qi00694b.
[24] El-Fakharany E.M., Sánchez L., Al-Mehdar H.A., Redwan E.M., Effectiveness of human, camel, bovine and sheep lactoferrin on the hepatitis C virus cellular infectivity: Comparison study, Virol. J. (2013). doi:10.1186/1743-422X-10-199.
[25] Mosmann T., Rapid colorimetric assay for cellular growth and survival: Application to proliferation and cytotoxicity assays, J. Immunol. Methods (1983). doi:10.1016/0022-1759(83)90303-4.
[26] Almahdy O., EL-Fakharany E.M., EL-Dabaa E., Ng T.B., Redwan E.M., Examination of the activity of camel milk casein against hepatitis C virus (Genotype-4a) and its apoptotic potential in hepatoma and HeLa cell lines, Hepat Mon. (2011). doi:10.5812/kowsar.1735143X.1367.
[27] Abu-Serie M.M., El-Fakharany E.M., Efficiency of novel nanocombinations of bovine milk proteins (lactoperoxidase and lactoferrin) for combating different human cancer cell lines, Sci. Rep. 7 (2017). doi:10.1038/s41598-017-16962-6.
[28] Uversky V.N., El-Fakharany E.M., Abu-Serie M.M., Almehdar H.A., Redwan E.M., Divergent Anticancer Activity of Free and Formulated Camel Milk α-Lactalbumin, Cancer Investig. (2017). doi:10.1080/07357907.2017.1373783.

[29] El-Fakharany E.M., Abu-Serie M.M., Litus E.A., Permyakov S.E., Permyakov E.A., Uversky V.N., Redwan E.M., The Use of Human, Bovine, and Camel Milk Albumins in Anticancer Complexes with Oleic Acid, Protein J. (2018). doi:10.1007/s10930-018-9770-1.
[30] El-Fakharany E.M., Abu-Elreesh G.M., Kamoun E.A., Zaki S., Abd-EL-Haleem D.A., In vitro assessment of the bioactivities of sericin protein extracted from a bacterial silk-like biopolymer, RSC Adv. (2020). doi:10.1039/c9ra09419a.
[31] Taha R.H., El-Shafiey Z.A., Salman A.A., El-Fakharany E.M., Mansour M.M., Synthesis and characterization of newly synthesized Schiff base ligand and its metal complexes as potent anticancer, J. Mol.Struct. (2019). doi:10.1016/j.molstruc. 2018.12.055.

Supporting information

Table S1: Analytical data and some physical properties of Schiff base ligand, and its complexes

Molecular formula (M.Wt)	**Colour**	**M.P(^{0}c)**	***Λ* m ***	**Elem. Anal . found (calcd.)**					
				C	**H**	**N**	**O**	**Cl**	**M**
HL	Orange	155	0.68	75.65	5.77	10.98	8.12	-------	-------
$C_{25}H_{23}N_3O_2$ (397.51)				(75.53)	(5.84)	(10.57)	(8.05)		
(1)[Co(HL)Cl $(H_2O)_3$]	Yellowish	170	7.42	54.08	4.99	7.42	13.97	7.88	11.72
$CoC_{25}H_{22}N_3O_2Cl(H_2O)_3$(54	green			(55.09)	(5.18)	(7.71)	(14.68)	(6.50)	(10.81)
4.95)									
(2)[Cd(HL)Cl.$(H_2O)_3$]	Yellowish	210	1.78	50.02	4.55	7.53	13.98	5.88	22.62
$CdC_{25}H_{22}N_3O_2Cl(H_2O)_3$	White			(50.17)	(4.72)	(7.02)	(13.36)	(5.92)	(18.78)
(598.42)									
(3)[La(HL)$(NO_3)_3(H_2O)$]	Yellow	188	7.17	44.23	3.65	10.67	23.78	--------	20.34
$LaC_{25}H_{22}N_3O_2(NO_3)_3$				(43.22)	(3.78)	(10.08)	(23.03)		(19.86)
$(H_2O)_2$ (694.56)									
(4) [Gd(HL)$(NO_3)_3(H_2O)$]	Yellow	195	1.58	42.76	3.55	10.09	22.98	-------	21.98
$GdC_{25}H_{22}N_3O_2(NO_3)_3$				(42.06)	(3.67)	(9.81)	(22.41)		(22.02)
$(H_2O)_2$ (713.81)									
(5) [Gd(HL)$(NO_3)_3(H_2O)$]	Yellow	115	1.50	41.62	3.24	9.19	22.38	-------	21.85
$GdC_{25}H_{22}N_3O_2(NO_3)_3$				(42.06)	(3.67)	(9.81)	(22.41)		(22.02)
$(H_2O)_2$ (713.81) (nano)									

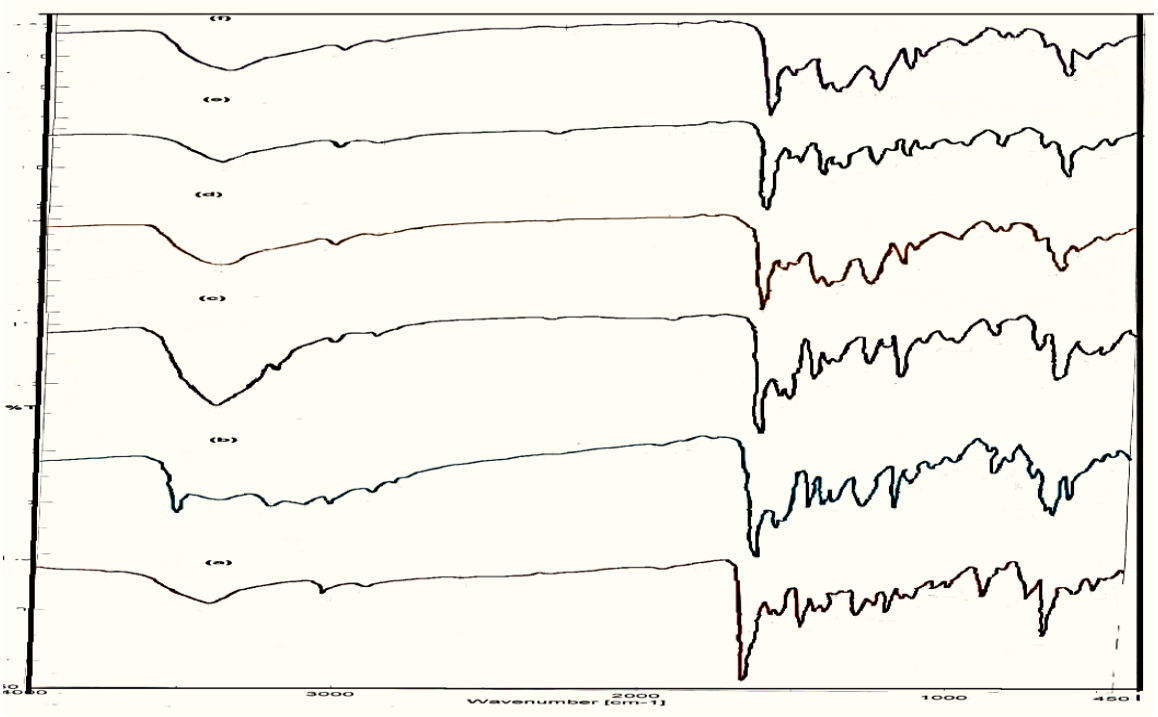

Fig.S1. IR spectrum analysis of (a) HL ligand, (b) complex of cobalt [Co(HL)Cl.3H_2O], (c) complex of cadmium [Cd(HL)Cl.3H_2O], (d) complex of lithium [La(HL)$(NO_3)_3$.H_2O], (e) complex of Gadolinium [Gd(HL)$(NO_3)_3$.H_2O] and (f) nano-complex of lithium [La(HL)$(NO_3)_3$.H_2O].

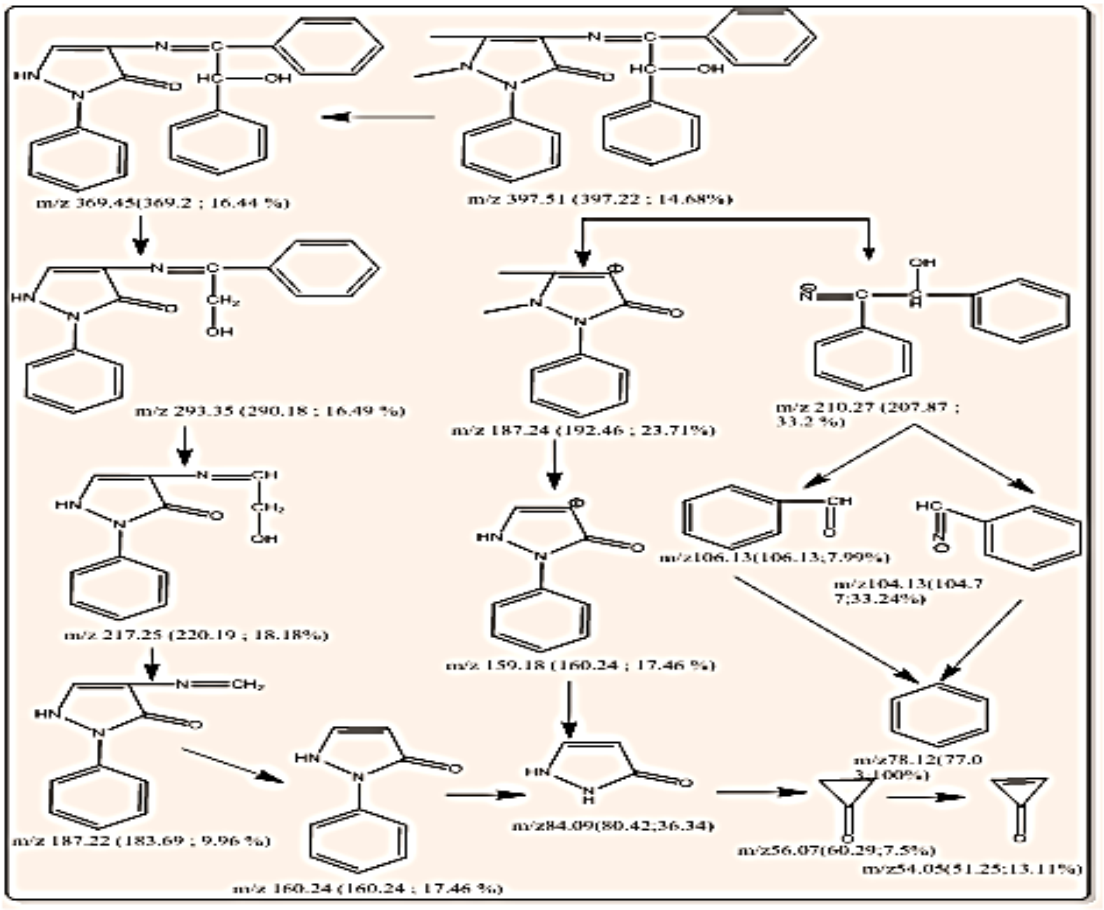

Fig.S2. Mass spectrum fragmentation pathway of the ligand (b).

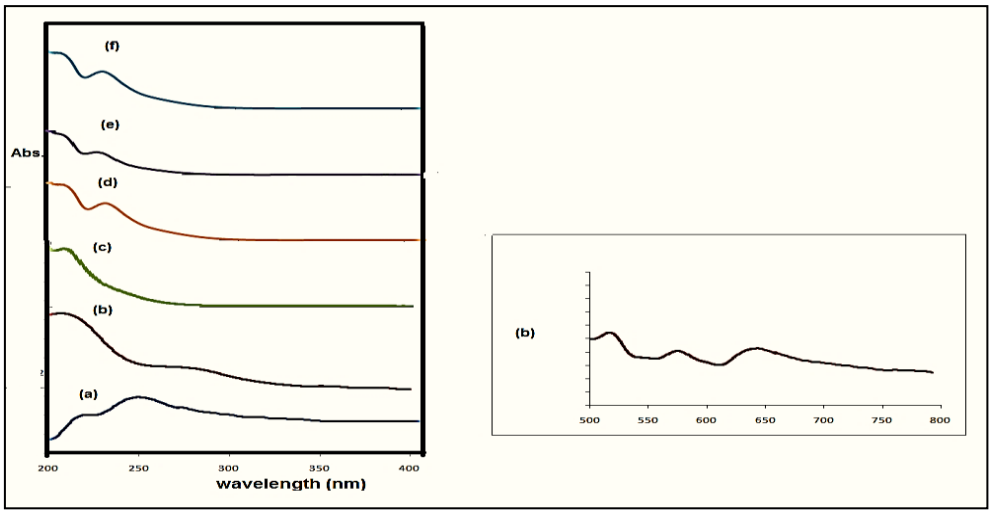

Fig.S3. UV spectra analysis of (a) HL ligand, (b) [Co(HL)(Cl).3H_2O], (c) [Cd(HL)(Cl).3H_2O], (d) [La(HL).(NO_3)$_3$.H_2O], (e) [Gd(HL).(NO_3)$_3$.H_2O] and (f) [Gd(HL).(NO_3)$_3$.H_2O] (nano).

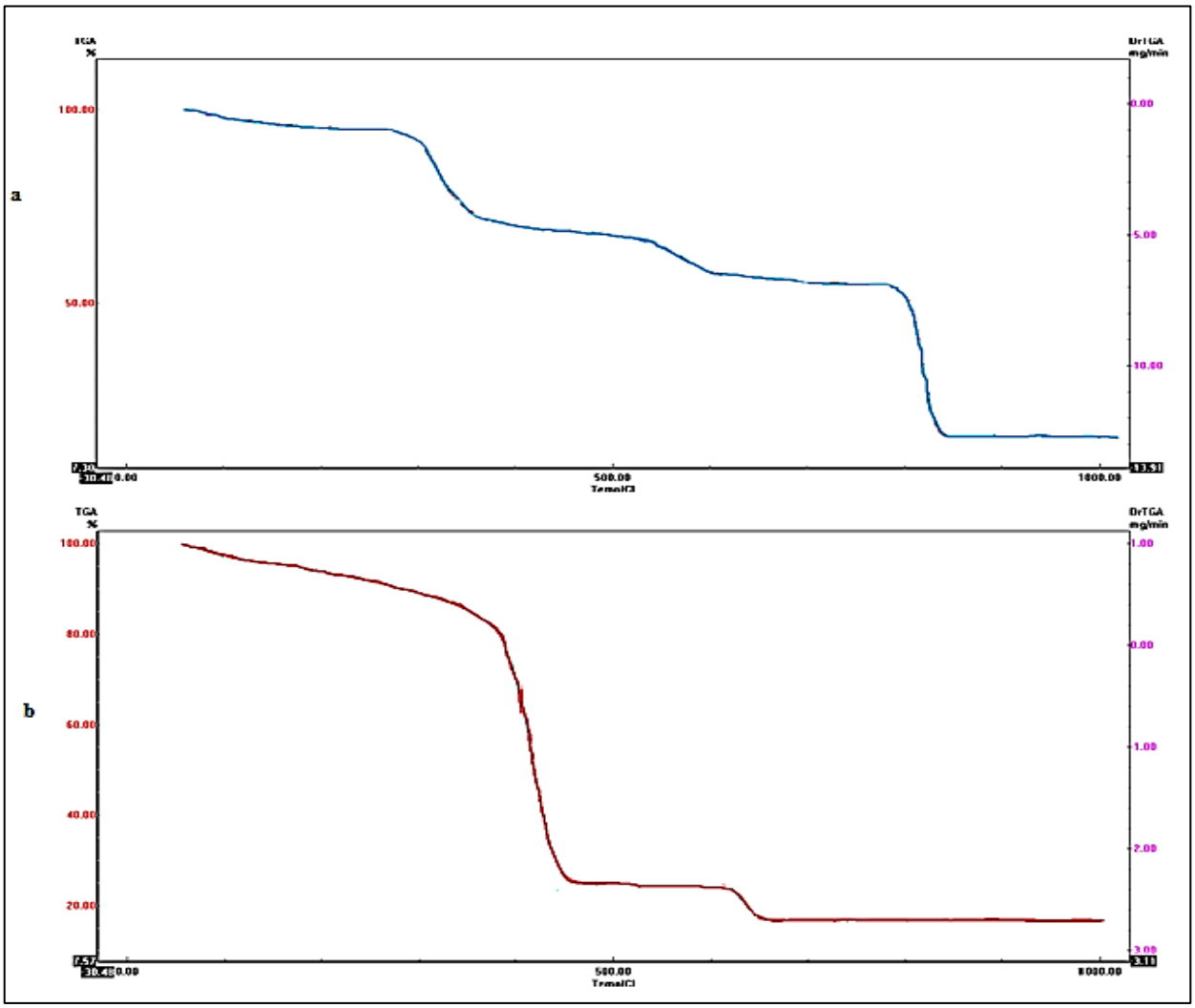

Fig.S4. TGA curve of (a) [Co(HL).Cl.3H_2O] complex and (b) TGA curve of the [La(HL).(NO_3)$_3$ .H_2O] complex.

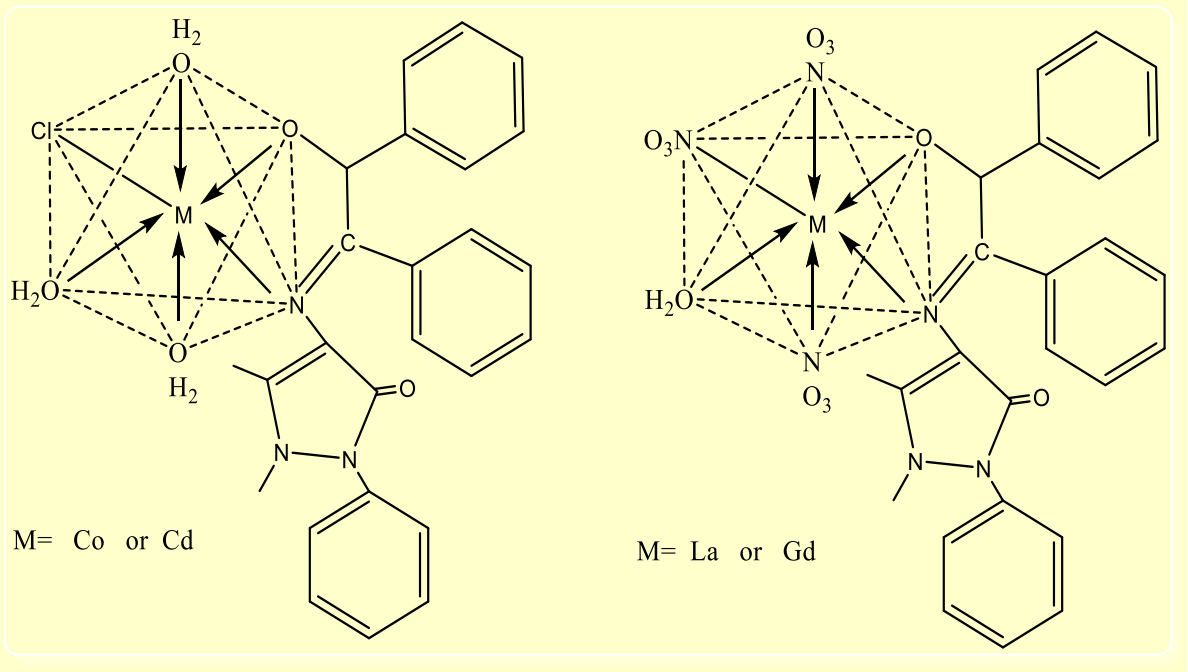

Fig.S5. Illustration represents the proposed structure of the metal complexes.